Polyhedron 122 (2017) 71–78

Contents lists available at ScienceDirect

Polyhedron

journal homepage: www.elsevier.com/locate/poly

New mixed-valence $Mn^{II}_4Mn^{IV}$ clusters from an unusual ligand transformation

Olajuyigbe A. Adebayo, Khalil A. Abboud, George Christou *

Department of Chemistry, University of Florida, Gainesville, FL 32611-7200, United States

ARTICLE INFO

Article history:
Received 8 September 2016
Accepted 14 October 2016
Available online 24 October 2016

Keywords:
Manganese
Crystal structure
Cluster
Magnetism
Hemiacetal

ABSTRACT

The syntheses, crystal structures and magnetic properties are reported of two new and unusual mixed-valence Mn clusters $[Mn^{II}_4Mn^{IV}O(mpko)_5(MeO\text{-}hmp)(mpko\text{-}hmp)(H_2O)](ClO_4)_3$ (**1**) and $[Mn^{II}_4Mn^{IV}O(ppko)_5(MeO\text{-}hmp)(ppko\text{-}hmp)(H_2O)](ClO_4)_3$ (**2**). They were obtained from the reaction of mpkoH or ppkoH and hmpH with $Mn(ClO_4)_2$ in the presence of NaOMe, where mpkoH is methyl(pyridin-2-yl)ketone oxime, ppkoH is phenyl(pyridin-2-yl)ketone oxime, and hmpH is 2-(hydroxymethyl)pyridine. Complex **1** possesses a distorted Mn^{II}_4 cubane core attached to an external Mn^{IV} by the O^{2-} ion. The peripheral ligation includes two unprecedented hemiacetal ligands formed *in situ* from the reaction of hmpH with MeOH or mpkoH/ppkoH. Solid-state dc and ac magnetic susceptibility measurements established that both **1** and **2** possess an $S = {}^7/_2$ ground state, which was confirmed by ac in-phase susceptibility data. Simulations of the $\chi_M T$ versus T data established the presence of dominant antiferromagnetic exchange interactions, rationalizing the observed ground state.

1. Introduction

Polynuclear clusters of 3d transition metals have been a major focus of scientific endeavor for many years, and for several reasons including the quest to understand the details of their roles in active sites of many enzymes, their relevance to research areas such as molecular magnetism, and not least the intrinsic structural beauty that they often exhibit [1–6]. Manganese clusters, in particular, continue to be under immense study because of the interesting magnetic properties they commonly display, such as Ising-type magnetoanisotropy (negative zero-field splitting parameter, D) as a consequence of Jahn–Teller (JT) axial elongation of Mn^{III} in near-octahedral geometry [7,8]. When this anisotropy is combined with large ground-spin state (S), it can result in a significant magnetization relaxation barrier, making them single-molecule magnets (SMMs) [9]. These are molecules that function as nanoscale magnets below their blocking temperature (T_B), and often display interesting quantum behaviors such as quantum tunneling of magnetization [10,11] and quantum phase interference [12–14] that make them candidates for potential applications in new technologies, such as qubits for quantum computation and molecular components of spintronics devices [15–17].

For a variety of such reasons, we continue to explore synthetic procedures to new manganese clusters. Of relevance to the present work is the rich variety of such species that we and other groups have reported from utilization of chelating/bridging ligands such as 2-(hydroxymethyl)pyridine (hmpH) and methyl(pyridin-2-yl) ketone oxime (mpkoH), either by themselves or in addition to carboxylate ligands [18–22]. Many clusters from these reactions, and analogous ones using bulkier derivatives of these chelates [23–30], have displayed interesting structures and/or magnetic properties, and some have turned out to be new single-molecule magnets (SMMs). The latter owes much to the propensity of bridging hmp^- to lead to ferromagnetic (**F**) coupling [18,21,31–34], as indeed do a number of oximate chelates in Mn cluster chemistry [20,35,36]. In addition, some of the Mn_3 SMMs have also proven excellent precursors for making supramolecular aggregates or high nuclearity manganese clusters [37–40].

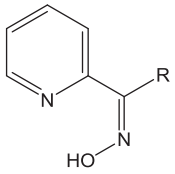

R = Me (mpkoH) or Ph (ppkoH)

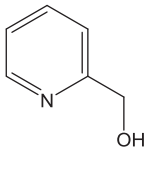

hmpH

* Corresponding author.
E-mail address: christou@chem.ufl.edu (G. Christou).

http://dx.doi.org/10.1016/j.poly.2016.10.018
0277-5387/

In the present work, we have explored the joint use hmpH and mpkoH together in non-carboxylate reactions in MeOH with simple Mn^{II} salts in the presence of base to encourage air oxidation of Mn^{II}; we anticipated that the combined use of these distinctly different chelates might give some interesting new clusters. We also employed for comparison purposes the analogous phenyl(pyridine-2-yl) ketone oxime (ppkoH). We herein report the synthesis, crystal structure and magnetochemical characterization of a new Mn_5 cluster type, which is unusual in multiple ways, namely its $Mn^{II}_4Mn^{IV}$ oxidation level involving Mn ions differing by two oxidation units, and the occurrence of two different chelates generated *in situ* from a transformation involving hemiacetal formation between hmpH and either MeOH or mpkoH.

2. Experimental

2.1. Synthesis

All preparations were performed under aerobic conditions using chemicals and solvents as received, unless otherwise stated. mpkoH [41] and ppkoH [42] were prepared as described. *Safety Note: perchlorates salts are potentially explosive and should be used in small quantities and handled with extreme care at all times.*

2.1.1. $[Mn^{II}_4Mn^{IV}O(mpko)_5(MeO\text{-}hmp)(mpko\text{-}hmp)(H_2O)](ClO_4)_3$ (**1**)

To a stirred solution of hmpH (0.60 mmol, 58 μL) in MeOH (25 mL) were added NaOMe (0.73 mmol, 0.050 g) and $Mn(ClO_4)_2\cdot 6H_2O$ (0.60 mmol, 0.22 g). Solid mpkoH (0.60 mmol, 0.080 g) was added to the resulting light brown solution, which rapidly turned deep brown. The solution was stirred for a further 60 min, filtered, and the filtrate allowed to stand undisturbed in a closed vial at ambient temperature. Dark brown X-ray quality crystals of **1**·*x*MeOH·*y*H_2O slowly grew over 18 h. They were collected by filtration, washed with MeOH, and dried under vacuum. The yield was 84% based on Mn. Elemental analysis: Calc. (Found) for **1**·2H_2O ($C_{55}H_{61}Cl_3Mn_5N_{14}O_{25}$): C, 38.88 (38.96); H, 3.62 (3.86); N, 11.54 (11.33); Cl 6.26 (5.92) %. Selected IR data (KBr, cm^{-1}): 3423(br), 2066(w), 1597(s), 1474(s), 1436(w), 1384(s), 1290(w), 1109(w), 1039(w), 866(s), 777(s), 707(s), 624(s), 544(s), 486(s).

2.1.2. $[Mn^{II}_4Mn^{IV}O(ppko)_5(MeO\text{-}hmp)(ppko\text{-}hmp)(H_2O)](ClO_4)_3$ (**2**)

To a stirred solution of hmpH, (0.60 mmol, 58 μL) in $CHCl_3$/MeOH (25 mL) were added NaOMe (0.73 mmol, 0.050 g) and $Mn(ClO_4)_2\cdot 6H_2O$ (0.60 mmol, 0.22 g). Solid ppkoH (0.60 mmol, 0.12 g) was added to the resulting light brown solution, which rapidly turned deep brown. The solution was stirred for a further 60 min, filtered, and the filtrate layered with pentane. Dark brown crystals slowly grew, and after 6 weeks were collected by filtration, washed copiously with pentane, and dried under vacuum. The yield was 63% based on Mn. Elemental analysis: Calc. (Found) for **2**·2H_2O ($C_{86}H_{76}N_{14}O_{25}Cl_3Mn_5$): C, 49.50 (49.56); H, 3.67 (4.04); N, 9.40 (9.27); Cl 5.10 (4.86) %. Selected IR data (KBr, cm^{-1}): 3423 (br), 2066(w), 1597(s), 1474(s), 1436(w), 1384(s), 1290(w), 1109 (w), 1039(w), 866(s), 777(s), 707(s), 624(s), 544(s), 486(s).

2.2. General and physical measurements

Elemental analyses (C, H, N, Cl) were performed by the in-house facilities of the University of Florida chemistry department and by Atlantic Microlab, Inc. Infrared spectra in the 400–4000 cm^{-1} range were recorded in the solid state (KBr pellets) on a Nicolet Nexus 670 FTIR Spectrometer. Variable-temperature dc and ac magnetic susceptibility data were collected using a Quantum Design MPMS-XL SQUID magnetometer equipped with a 7 T dc magnet. Pascal's constants were used to estimate the diamagnetic corrections, which were subtracted from the experimental susceptibilities to give the molar magnetic susceptibilities (χ_m) [43]. Microcrystalline samples were restrained in eicosane to avoid torquing.

2.2.1. X-ray Crystallography

Data for **1**·*x*MeOH·*y*H_2O were collected at 100 K on a Bruker DUO diffractometer using MoK_α radiation (λ = 0.71073 Å) and an APEXII CCD area detector. Raw data frames were read by program SAINT [44] and integrated using 3D profiling algorithms. The resulting data were reduced to produce hkl reflections and their intensities and estimated standard deviations. The data were corrected for Lorentz and polarization effects, and numerical absorption corrections were applied based on indexed and measured faces. The structure was solved and refined in SHELXTL6.1, using full-matrix least-squares refinement on F^2. The non-H atoms were refined with anisotropic thermal parameters and all of the H atoms were placed in calculated, idealized positions and refined riding on their parent atoms.

The asymmetric unit consists of two Mn_5 cluster cations (**A** and **B**), six ClO_4^- anions, and approximately thirteen MeOH and three H_2O solvent molecules. In Mn_5 cation **A**, the H atoms of the coordinated H_2O molecule (O11A) were located in a difference Fourier map and were refined as riding on their parent atom. In the Mn_5 cation **B**, the H_2O is replaced by a disordered MeOH ligand (O11B and C) and its partial H atoms were placed in calculated positions. Of the six ClO_4^- anions, only the Cl1 anion was not disordered; the others were disordered to different extents. The anions with Cl2 and Cl4 both were disordered about two positions sharing three of the O atoms. The Cl3 anion was fully disordered and refined in two parts. The Cl5 anion showed some disorder with a nearby MeOH molecule. The final model also included several partial MeOH and H_2O molecules scattered around voids in the lattice. In the final refinement cycle, 36,041 reflections (of which 17,235 were observed with $I > 2\sigma(I)$) were used to refine 2003 parameters, and the resulting R_1, wR_2 and S (goodness of fit) were 7.17%, 20.36% and 1.117, respectively. Selected crystal data and refinement parameters are listed in Table 1.

3. Results and discussion

3.1. Synthesis

The reaction of $Mn(ClO_4)_2$, hmpH, and mpkoH in a 1:1:1 molar ratio in MeOH with 1.2 equiv of NaOMe resulted in a deep brown

Table 1
Unit cell and structure refinement parameters for **1**·*x*MeOH·*y*H_2O.

Formula[a]	$C_{55}H_{57}Cl_3Mn_5N_{14}O_{23}$
FW (g/mol)[a]	1663.21
Crystal system	triclinic
Space group	$P\bar{1}$
a (Å)	16.7793(11)
b (Å)	20.3974(14)
c (Å)	25.0501(17)
α (°)	75.024(1)
β (°)	74.939(1)
γ (°)	75.607(1)
V (Å^3)	7845.1(9)
z	2
T (K)	100(2)
λ (Å)[b]	0.71073
ρ_{cal} (mg/m^3)	1.562
μ (mm^{-1})	1.386
R_1[c,d]	0.1631
wR_2[e]	0.2329

[a] Excluding lattice solvent molecules.
[b] Graphite monochromator.
[c] $I > 2\sigma(I)$.
[d] $R1 = 100\Sigma(||F_o| - |F_c||)/\Sigma|F_o|$.
[e] $wR_2 = 100[\sum [w(F_o^2 - F_c^2)^2]/\sum[w(F_o^2)^2]]^{1/2}$, $w = 1/[\sum^2(F_o^2) + [(ap)^2 + bp]$, where $p = [\max(F_o^2, O) + 2F_c^2]/3$; a and b are constants.

solution indicating air-oxidation of Mn^{2+}, and subsequent isolation of X-ray quality crystals of **1**·*x*MeOH·yH_2O in 84% yield. Small changes to the amount of mpkoH or hmpH still gave the same product in comparable yield. **1** was also obtained, but in a decreased yield of 56%, when NaOMe was replaced with NEt_3. When $Mn(NO_3)_2$ or $MnCl_2$ were used, we could not isolate any pure material for characterization. If mpkoH was omitted, a previously reported Mn_4 complex [45] was obtained.

Once the crystal structure of **1** had been determined (vide infra), it became obvious that some interesting organic transformations had occurred *in situ* leading to two distinct hemiacetals being formed and acting as chelating ligands on the cluster. The two hemiacetals are methoxy(pyridine-2-yl)methanol (MeO-hmpH) and (E)-1-(pyridin-2-yl) ethan-1-one O-(hydroxy(pyridin-2-yl) methyl) oxime (mpko-hmpH), abbreviated to reflect their clear derivation from the indicated groups. On the basis of the usual pathway for hemiacetal formation being attack by an alcohol on an aldehyde, we propose the pathways in Scheme 1 for the formation of MeO-hmp$^-$ and mpko-hmp$^-$. The Mn-assisted air oxidation of hmpH to 2-formylpyridine is proposed as the first step, followed by attack on the carbonyl by MeOH or mpkoH. We omit any metal ions from the scheme, although it is likely that binding to Lewis-acidic $Mn^{2+/3+}$ ions activates the hmpH to oxidation and the 2-formylpyridine to reaction, the latter being analogous to the general use of acidic media to activate aldehydes to hemiacetal formation by protonating the carbonyl O atom. The resulting MeO-hmp$^-$ and mpko-hmp$^-$ would then be trapped by their binding to Mn ions and stabilized to the reverse reactions, which are facile except in cyclic hemiacetals [46]; the binding modes to the Mn atoms are described below (vide infra). The formation of MeO-hmp$^-$ is reasonable given the large amount of MeOH present, whereas the formation of mpko-hmp$^-$ is a little surprising for the same reason. The formation of **1** is summarized in Eq. (1):

$$5Mn^{2+} + 6mpkoH + 2hmpH + MeO^- + O_2 \rightarrow [Mn^{II}_4Mn^{IV}O(mpko)_5(MeO-hmp)(mpko-hmp)(H_2O)]^{3+} + 6H^+ \quad (1)$$

Note that the oxidation of hmp$^-$ to picolinate (pic$^-$; pyridine-2-carboxylate) has been previously observed in the synthesis of $[Mn_{21}O_{16}(O_2CMe)_{16}(hmp)_6(hmpH)_2(pic)_2(py)(H_2O)]^{4+}$ salts [47], and since the reaction very likely proceeded via a 2-formylpyridine intermediate, it provides some precedent for postulating the same intermediate in the present hemiacetal formations.

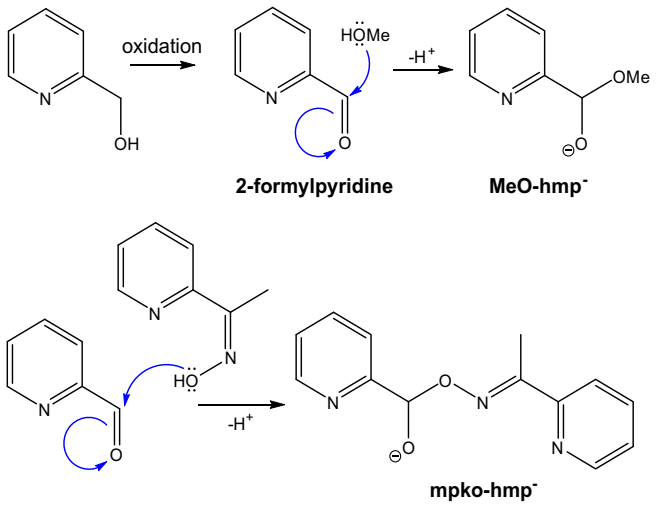

Scheme 1. Proposed steps in the conversion of hmpH to the anions of (top) methoxy(pyridine-2-yl)methanol (MeO-hmpH), and (bottom) (E)-1-(pyridin-2-yl) ethan-1-one O-(hydroxy(pyridin-2-yl)methyl) oxime (mpko-hmpH).

With **1** structurally identified, we also employed ppkoH instead of mpkoH in the same reaction, hoping the Ph-for-Me substitution would divert the reaction to a different product. However, the IR spectrum, elemental analysis, and magnetic properties (vide infra) of the resulting complex **2** indicated it to be structurally analogous to **1**.

3.2. Structural description of $[Mn_5O(mpko)_5(MeO\text{-}hmp)(mpko\text{-}hmp)(H_2O)]^{3+}$

There are two inequivalent but near-superimposable Mn_5 cations (**A** and **B**) in the asymmetric unit, and only the former (with atom labels ending in A) will be described. The labeled core and a stereopair of the complete cation are shown in Fig. 1, and selected interatomic distances and angles are listed in Table 2. The cation possesses a low-symmetry $\{Mn^{II}_4(\mu_4\text{-}O^{2-})(\mu_3\text{-}OR)_2(\mu_3\text{-}NO)\}$ cuboidal core, with the oxide ion (O1A) becoming μ_4 with near-tetrahedral geometry by attaching to the external Mn^{IV} atom, Mn4A. Alternatively, the structure can be described as a tetrahedral $\{Mn_4(\mu_4\text{-}O^{2-})\}$ unit to which is attached Mn5A via three alkoxide O atoms; this description will be useful in the magnetism discussion below. The Mn oxidation states were apparent from the metric parameters, and confirmed by bond valence sum calculations (Table 3). As expected, the Mn^{IV} atom Mn4A is six-coordinate octahedral, as are two of the Mn^{II} atoms, Mn1A and Mn2A. The other two Mn^{II} atoms, Mn3A and Mn5A, are seven-coordinate. The five Mn atoms form a trigonal bipyramid with the Mn^{IV} on the axis.

The two μ_3-RO$^-$ in the core are the alkoxides of the MeO-hmp$^-$ and mpko-hmp$^-$ groups, whose complete Mn binding modes are shown in Scheme 2 and Fig. S1. Also shown is the ligation mode of the five mpko$^-$ chelates, which are in their usual chelating/bridging modes. It is interesting to note that there are no hmp$^-$ ligands in **1**, only their hemiacetal derivatives. Finally, the peripheral ligation is completed by one terminal water molecule.

The type of ligand transformation seen in this work is by no means unprecedented in metal-oxo cluster chemistry. Perlepes and coworkers have encountered a large variety of transformations of organic ketones, such as di-2-pyridyl ketone $(py)_2CO$, 2-acetylpyridine (py)(Me)CO and others, into metal-stabilized deprotonated forms of the gem-diols or hemiketals, i.e., $(py)_2C(OH)_2$ and $(py)_2C(OH)(OR)$, etc., from nucleophilic attack by water or alcohol, respectively [48]. These have led to 3d metal clusters with a wide range of metal nuclearities and structural topologies. In our own work, we have previously encountered an unusual hemiacetyl group LH_3 formed *in situ* and bound as a pentadentate LH^{2-} chelate from the reaction of $[Mn_3O(O_2CEt)_6(py)_3][ClO_4]$ with pyrine-2,6-dimethanol ($pdmH_2$) in MeCN [49]. We proposed that oxidation of one of the hydroxymethyl arms of $pdmH_2$ to the corresponding aldehyde had occurred, followed by nucleophilic attack by a second $pdmH_2$ group; this would thus be similar to the formation of mpko-hmp$^-$ by attack of mpko$^-$ on 2-formylpyridine.

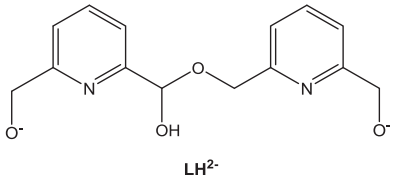

Finally, complexes **1** and **2** form new additions to the family of Mn_5 clusters known to date. These are collected in Table 4 together with their core topologies and ground state spin values.

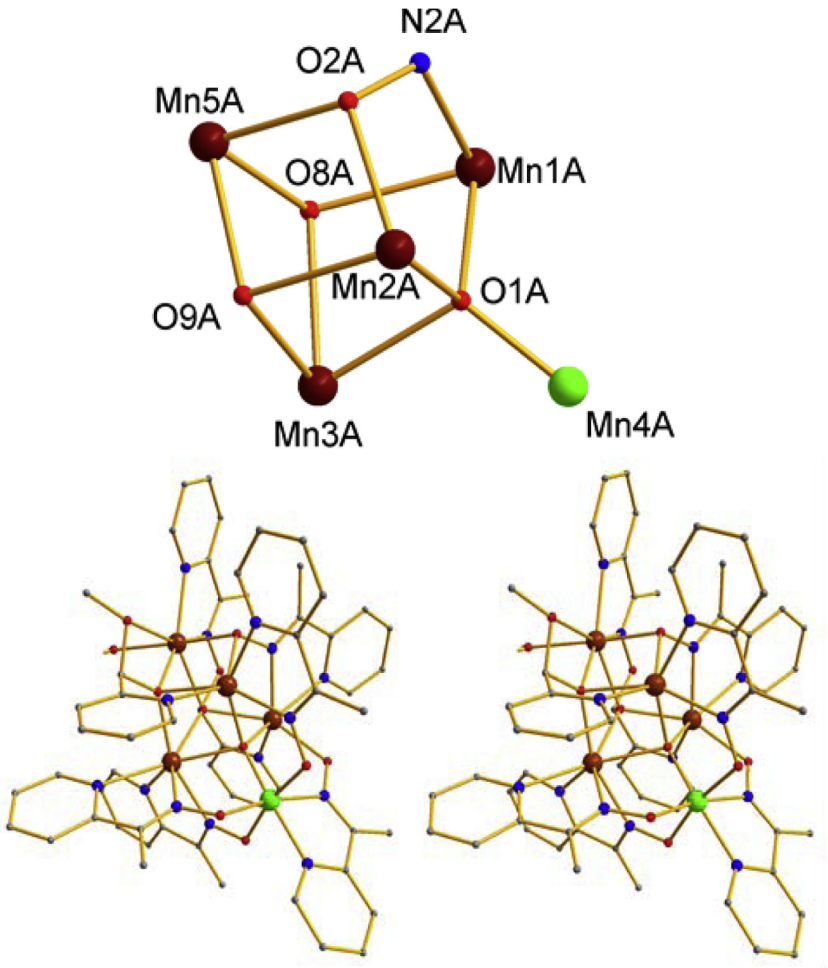

Fig. 1. (Top) Labeled core of cation **A** of **1**, and (bottom) a stereopair of the complete cation. Color code: Mn^{IV} green, Mn^{II} brown, N blue, O red, C gray. (For interpretation of the references to color in this figure legend, the reader is referred to the web version of this article.)

Table 2
Selected bond distances (Å) and angles (°) for complex **1**.[a]

Mn(1)–O(6)	2.099(4)	Mn(3)–N(8)	2.336(5)
Mn(1)–O(1)	2.167(4)	Mn(3)–O(8)	2.400(4)
Mn(1)–N(2)	2.197(5)	Mn(3)–N(7)	2.423(5)
Mn(1)–N(1)	2.230(5)	Mn(4)–O(1)	1.779(4)
Mn(1)–O(8)	2.240(4)	Mn(4)–O(5)	1.889(4)
Mn(1)–N(1)	2.328(5)	Mn(4)–O(3)	1.909(4)
Mn(2)–O(2)	2.117(4)	Mn(4)–O(4)	1.921(4)
Mn(2)–O(1)	2.150(4)	Mn(4)–N(10)	2.028(5)
Mn(2)–N(4)	2.201(5)	Mn(4)–N(9)	2.053(5)
Mn(2)–N(14)	2.211(5)	Mn(5)–O(9)	2.154(4)
Mn(2)–N(3)	2.262(5)	Mn(5)–O(2)	2.194(4)
Mn(2)–O(9)	2.331(4)	Mn(5)–O(11)	2.228(4)
Mn(3)–O(9)	2.143(4)	Mn(5)–N(12)	2.238(5)
Mn(3)–N(6)	2.215(5)	Mn(5)–O(8)	2.242(4)
Mn(3)–O(1)	2.275(4)	Mn(5)–N(11)	2.269(5)
Mn(3)–N(5)	2.297(5)		
Mn(4)–O(1)–Mn(2)	117.3(2)	Mn(1)–O(8)–Mn(5)	112.13(16)
Mn(4)–O(1)–Mn(1)	116.23(19)	Mn(1)–O(8)–Mn(3)	98.09(15)
Mn(2)–O(1)–Mn(1)	109.24(17)	Mn(5)–O(8)–Mn(3)	97.77(15)
Mn(4)–O(1)–Mn(3)	111.21(18)	Mn(3)–O(9)–Mn(5)	108.99(17)
Mn(2)–O(1)–Mn(3)	96.04(14)	Mn(3)–O(9)–Mn(2)	94.61(15)
Mn(1)–O(1)–Mn(3)	104.20(16)	Mn(5)–O(9)–Mn(2)	96.60(15)

[a] For cation **A** of the two independent cations in the asymmetric unit, the one with atom labels ending with A in the cif; for convenience, the A suffix has been omitted from all atoms in the Table.[b]

Table 3
Bond valence sums for Mn atoms in **1**.

Atom	Mn(II)	Mn(III)	Mn(IV)
Mn1A	2.04	1.92	1.93
Mn2A	2.04	1.93	1.93
Mn3A	1.94	1.84	1.83
Mn4A	4.20	3.91	4.00
Mn5A	1.90	1.77	1.80

The oxidation state is the nearest whole number to the underlined value, which is the one closest to the value with which it was calculated.

3.3. Magnetic susceptibility studies

3.3.1. Dc susceptibility studies

Variable-temperature, solid-state magnetic susceptibility data in a 0.1 T dc field and in the 5.0–300 K range were collected on powdered microcrystalline samples of **1**·2H_2O and **2**·2H_2O restrained in eicosane to prevent torquing. The data are shown as $\chi_M T$ versus T plots in Fig. 2, and the two complexes are seen to exhibit similar overall profiles. The $\chi_M T$ increase with decreasing T from 15.03 to 15.64 $cm^3\,K\,mol^{-1}$ at 300 K to maxima of 18.22 $cm^3\,K\,mol^{-1}$ at 40 K and 17.44 $cm^3\,K\,mol^{-1}$ at 50 K, for **1**·2H_2O and **2**·2H_2O, respectively, and then decrease to 11.02 and

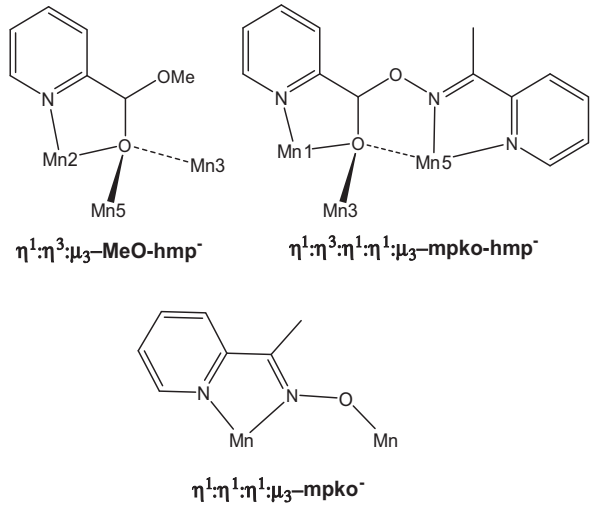

Scheme 2. Ligation modes of the MeO-hmp$^-$, mpko-hmp$^-$ and five mpko$^-$ chelates in the cation of **1**. The metal atom labeling is that for cation **A**.

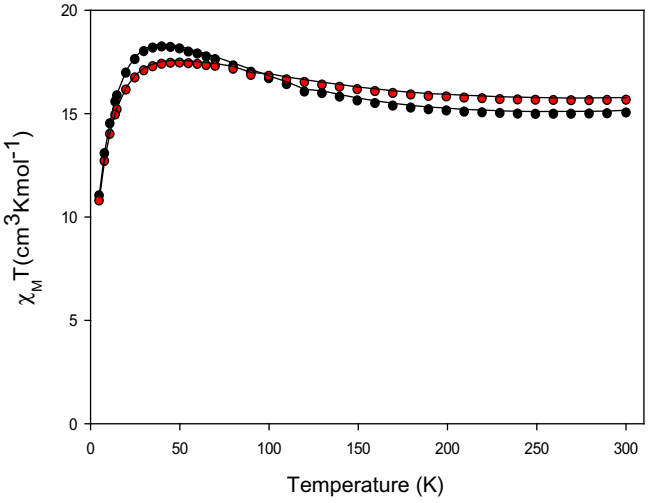

Fig. 2. $\chi_M T$ vs. T plots for **1**·2H$_2$O (●) and **2**·2H$_2$O (●).

10.77 cm^3 K mol^{-1} at 5.0 K. The 300 K values are less than the spin-only (g = 2) $\chi_M T$ of 19.38 cm^3 K mol^{-1} for 4Mn^{II}Mn^{IV} non-interacting ions, indicating the increase in $\chi_M T$ with decreasing T to be due to ferrimagnetic spin alignments from antiferromagnetic (**AF**) interactions rather than dominant ferromagnetic (**F**) ones, with the decrease at the lowest temperatures assignable to additional weak **AF** interactions. This would be consistent with the fact that Mn^{II}Mn^{II} exchange interactions are usually **AF**, as are those involving Mn^{IV}. There may be some contributions from intermolecular interactions and zero-field splitting to the decreases in $\chi_M T$ at the lowest temperatures, but since we saw no significant inter-cation interactions in the crystal structure, and high-spin Mn^{II} and Mn^{IV} are both electronically isotropic ions, we expect such contributions to be minimal.

The lowest T data suggest a significant non-zero ground state spin. The low-symmetry of the cations, the large number ($\geqslant$5) of inequivalent exchange interactions (J_{ij}), and the many expected very weak Mn^{II}Mn^{II} interactions, prevent derivation using the Kambe method [63] of a Van Vleck equation to fit the data. In any case, a high density of low-lying excited states was expected from the weak Mn^{II}Mn^{II} interactions, and for all these reasons we decided to determine the ground state using ac susceptibility methods, and estimate the constituent pairwise Mn$_2$ J_{ij} values using MAGPACK [64].

Table 4
Structural types and ground state S values for Mn$_5$ clusters.

Complex[a,b]	Core	Type[c–i]	S	Ref.
$[Mn^{II}_5(Htrz)_2(SO_4)_4(OH)_2]$	$[Mn_5(\mu_3\text{-}OH)_2]^{8+}$	c	n.r.	[50]
$[Mn^{II}_5(poapH)_6]^{4+}$	$[Mn_5(\mu\text{-}OR)_6]^{4+}$	d	$^5/_2$	[51]
$[Mn^{II}_5(poapH)_6]^{4+}$	$[Mn_5(\mu\text{-}OR)_6]^{4+}$	d	$^5/_2$	[51]
$[Mn^{II}_5(L)_2(O_2CMe)_2(ClO_4)_2]^{2+}$	$[Mn_5(\mu\text{-}OR)_6(\mu\text{-}OClO_3)_2]^{2+}$	e	n.r.	[52]
$[Mn^{II}_5(phaapH)_6]^{4+}$	$[Mn_5(\mu\text{-}OR)_6]^{4+}$	d	$^5/_2$	[53]
$[Mn^{III}_5O_3(^tBuPO_3)_2(O_2CMe)_5(H_2O)(phen)_2]$	$[Mn_5(\mu_3\text{-}O)_3]^{9+}$	i	2	[54]
$[Mn^{III}_5O_3(^tBuPO_3)_2(O_2CPh)_5(phen)_2]$	$[Mn_5(\mu_3\text{-}O)_3]^{9+}$	i	2	[54]
$[Mn^{II}_5(\mu_3\text{-}O)_2(L'_1)_4(O_2CMe)_3(MeOH)]$	$[Mn_5(\mu_3\text{-}O)_2(\mu\text{-}OR)_5]^{6+}$	i	2	[55]
$[Mn^{II}_5(\mu_3\text{-}O)_2(L'_1)_4(O_2CPh)_3(MeOH)]$	$[Mn_5(\mu_3\text{-}O)_2(\mu\text{-}OR)_5]^{6+}$	i	2	[55]
$[Mn^{II}Mn^{III}_4(HL'_2)_2(L'_2)_2(O_2CMe)_4)]$	$[Mn_5(\mu\text{-}OR)_6]^{8+}$	e	2	[55]
$[Mn^{II}Mn^{III}_4(HL'_2)_2(L'_2)_2(O_2CPh)_4)]$	$[Mn_5(\mu\text{-}OR)_6]^{8+}$	e	2	[55]
$[Mn^{II}Mn^{III}_4(shi)_4(O_2CMe)(DMF)_6]$	$[Mn_5(\mu_3\text{-}ON)_4]^{10+}$	f	n.r.	[56]
$[Mn^{II}Mn^{III}_4(shi)_4(O_2CPh)_2(MeOH)_6]$	$[Mn_5(\mu_3\text{-}ON)_4]^{10+}$	f	n.r.	[57]
$[Mn^{II}_2Mn^{III}_3O(salox)_3Cl_2(N_3)_6]^{3-}$	$[Mn_5(\mu_3\text{-}O)(\mu\text{-}ON)_3(\mu\text{-}N_3)_6]^{2+}$	d	11	[58]
$[Mn^{II}_2Mn^{III}_3(LH_2)_3(LH_5)(MeOH)_3]^{4+}$	$[Mn_5(\mu\text{-}OR)_7]^{6+}$	d	2	[59]
$[Mn^{II}_3Mn^{III}_2(fsatren)_2(H_2O)_4]$	$[Mn_5(\mu\text{-}OR)_8]^{4+}$	g	$^7/_2$	[60]
$[Mn^{II}_3Mn^{III}_2(tmphen)_6(CN)_{12}]$	$Mn_5(\mu\text{-}NC)_6]^{6+}$	d	$^{11}/_2$	[61]
$[Mn^{II}_4Mn^{III}(cat)_4(O_2CBu^t)_2(py)_8\ ]^+$	$[Mn_5(\mu_3\text{-}OR)4(\mu\text{-}OR)_4]^{3+}$	e	n.r.	[62]
{$Mn^{II}_4Mn^{IV}$}$^{3+}$cation of **1**	$[Mn_5(\mu_4\text{-}O)(\mu\text{-}ONR)_7]^{3+}$	d	$^7/_2$	t.w
{$Mn^{II}_4Mn^{IV}$}$^{3+}$ cation of **2**	$[Mn_5(\mu_4\text{-}O)(\mu\text{-}ONR)_7]^{3+}$	d	$^7/_2$	t.w

[a] *Abbreviations:* Htrz = triazole; phaapH = ditopic, diazine ligands; LH_2 = [2 + 2] macrocycle; $H_2L'1$ = 3,5-dibromosalicylidene-2-ethanolamine; L′2 H2 = 3-(2-hydroxy-3,5-dibromobenzylideneamino)propane-1,2-diol; shiH3 = salicylhydroxamic acid; DMF = dimethylformamide, saloxH2 = salicylaldoxime; fsatrenH6 = 3-formylsalicylic acid; tmphen = 3,4,7,8-tetramethyl-1,10-phenanthroline; $catH_2$ = catechol; py = pyridine.
[b] Counterions and solvent molecules are omitted.
[c] Edge-sharing MnO_6 octahedra.
[d] Trigonal bipyramid.
[e] Four Mn around a central Mn.
[f] Four [12-metallacrown-4] ~Mn ring.
[g] Linear array.
[h] Basket-like cage.
[i] Incomplete cubane extended at one face by an incomplete adamantane unit. n.r. = not reported; t.w. = this work.

3.3.2. Ac susceptibility studies

In-phase ($\chi'_M T$) and out-of-phase (χ''_M) ac magnetic susceptibility data in the 1.8–15.0 K temperature range were collected on **1**·2H$_2$O and **2**·2H$_2$O using a 3.5 G ac field with oscillation frequencies in the 50–1000 Hz range. The in-phase data are plotted as $\chi'_M T$ versus T in Fig. 3 and exhibit steep decreases with decreasing T from 17.52 and 16.88 cm^3 K mol^{-1} to 9.55 and 9.27 cm^3 K mol^{-1} at 1.8 K. This is consistent with depopulation of low-lying excited states with spin S greater than that of the ground state, as expected for very weak **AF** interactions. Extrapolation of the data to 0 K, at which temperature only the ground state would be populated, gives $\chi'_M T$ slightly less than 8.0 cm^3 K mol^{-1}, indicating an $S = {}^7/_2$ ground state with $g \approx 2.0$; spin-only $\chi'_M T$ values for $S = {}^9/_2$, ${}^7/_2$ and ${}^5/_2$ systems are 12.38, 7.88 and 4.38 cm^3 K mol^{-1}. Neither complex exhibited out-of-phase χ''_M signals down to 1.8 K.

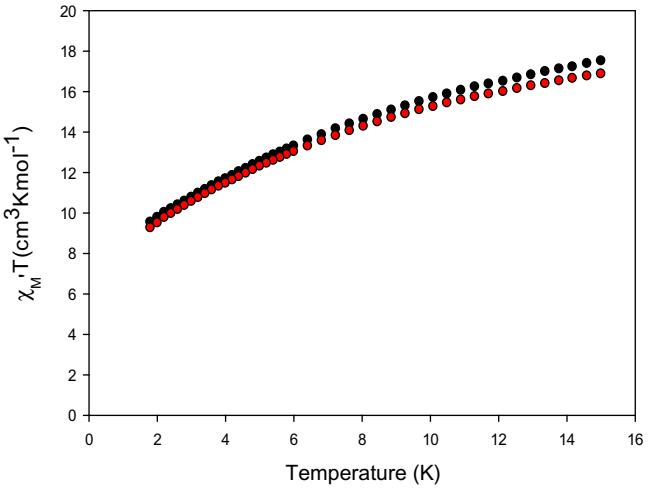

Fig. 3. In-phase ac $\chi'_M T$ vs. T plots at 1000 Hz for complexes **1**·2H$_2$O (●) and **2**·2H$_2$O (●).

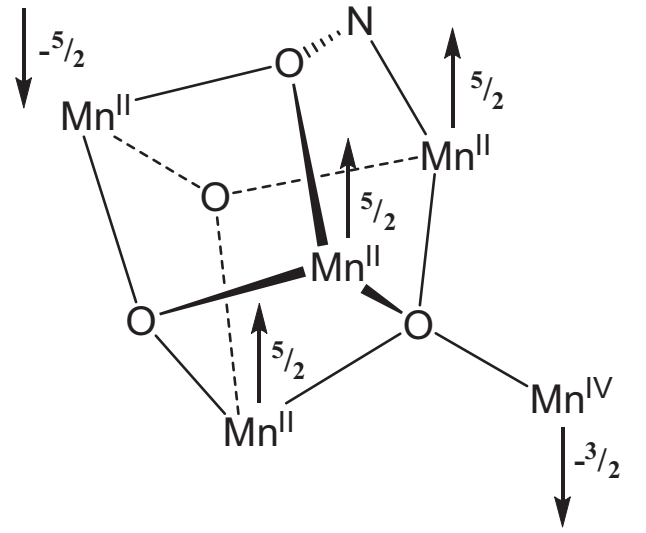

Fig. 4. Proposed ground state spin vector alignments in **1**·2H$_2$O and **2**·2H$_2$O leading to their observed $S = {}^7/_2$ ground states.

Assuming as a first approximation that the magnetic core has virtual C_3 symmetry, the spin Hamiltonian is given by Eq. (2), where the S_i subscripts refer to the atom labels of Fig. 1, and

$$\hat{H} = -2J_a(\hat{S}_1 \cdot \hat{S}_4 + \hat{S}_2 \cdot \hat{S}_4 + \hat{S}_3 \cdot \hat{S}_4) - 2J_b(\hat{S}_1 \cdot \hat{S}_2 + \hat{S}_2 \cdot \hat{S}_3 + \hat{S}_1 \cdot \hat{S}_3) - 2J_c(\hat{S}_1 \cdot \hat{S}_5 + \hat{S}_2 \cdot \hat{S}_5 + \hat{S}_3 \cdot \hat{S}_5) \quad (2)$$

$J_a = J$ (Mn^{IV}Mn^{II}), $J_b = J$ (Mn^{II}Mn^{II}) for Mn$^{II}_2$ pairs bridged by O^{2-}, and $J_c = J$ (Mn^{II}Mn^{II}) for Mn$^{II}_2$ pairs that include Mn5A. Excellent simulations using all the data were obtained (solid lines in Fig. 2) with $J_a = -9.2$ cm^{-1}, $J_b = -1.4$ cm^{-1}, and $J_c = -0.6$ cm^{-1} for **1**·2H$_2$O, and $J_a = -8.6$ cm^{-1}, $J_b = -1.7$ cm^{-1}, and $J_c = -0.4$ cm^{-1} for **2**·2H$_2$O, in both cases with g kept fixed at 2.0.

A ground state $S = {}^7/_2$ can readily be rationalized from these **AF** exchange interactions and the relative ordering $|J_a| > |J_b| \approx |J_c|$, i.e. $|J_{24}| > |J_{22}|$. The strongest J_{24} interactions would then align the Mn^{IV} spin vector antiparallel to those of the Mn^{II} ions bridged to it by the O^{2-} ion, overcoming (frustrating) the weaker J_b interactions with which it is competing (Fig. 4). This leads to the increase in $\chi_M T$ with decreasing T, until the weakest (alkoxide-bridged) J_c interactions to the distant Mn^{II} (Mn5A) align that spin vector antiparallel to the other Mn^{II} vectors, giving the overall $S = {}^{15}/_2 - {}^8/_2 = {}^7/_2$ ground state. This alignment of spin vectors in the ground state is shown in Fig. 4.

In Table 5, we compare the present results with those for the handful of other Mn^{II}/Mn^{IV} complexes that have been characterized magnetically. Except for two complexes for which unusually strong J values were reported, the general trend is that Mn^{II}Mn^{II} and Mn^{II}Mn^{IV} interactions are weak, as is typical for Mn^{II}. As such, the structural details at the bridging ligands (i.e., the type of bridging ligand, Mn-O-Mn angles, etc) will then determine whether the J values are weakly **F** or **AF**. Note that the two Mn$^{II}_3$Mn^{IV}O complexes contain a μ_4-O^{2-}-centered Mn$_4$ tetrahedron as found in **1**, and thus their $S = 6$ ground state is consistent with their spins being aligned as shown for the corresponding fragment of **1** in Fig. 4. Also, the three J_c interactions in **1** and **2** must be overall **AF** on average, to give the low-T drop in $\chi_M T$ as the Mn5A spin vector aligns antiparallel to those of the other Mn^{II}. Since one Mn^{II}Mn^{II} pair is bridged by an oximate group rather than an alkoxide, however, we wondered whether this might be weakly **F** instead of **AF**, as seen for several of the

Table 5
Exchange constants[a] and ground state S values for Mn^{II}Mn^{IV} complexes.

Complex[b]	S	J (Mn^{II}Mn^{II})[a]	J(Mn^{II}Mn^{IV})[a]	Ref.
[Mn$^{II}_2$Mn^{IV}(OMe)$_2$(mpko)$_4$Br$_2$]	${}^{13}/_2$	+0.3	+3.4	[65]
[Mn$^{II}_2$Mn$^{IV}_2$O$_2$(heed)$_2$(EtOH)$_6$Br$_2$]	0	−1.5	−11.8	[66]
[Mn$^{II}_2$Mn$^{IV}_2$(μ_4-Hedte)$_2$(thme)$_2$]	8	+3.97	+1.46	[67]
[Mn$^{II}_3$Mn^{IV}O(pko)$_4$(3,4-dpa)$_4$]	6	+2.1	−24.2, −1.33	[68]
[Mn$^{II}_3$Mn^{IV}O(N$_3$)(O$_2$CPh)$_3$(Ph(Py)CNO)$_4$]	6	+1.5, +0.8	−26.9, −1.75	[69]
[Mn$^{II}_4$Mn$^{IV}_3$(tea)(teaH$_2$)$_3$(peolH)$_4$]$^{2+}$	${}^{23}/_2$	+0.21	-0.35,+1.75	[70]
[Mn$^{II}_{24}$Mn$^{IV}_8$(thme)$_{16}$(bpy)$_{24}$(N$_3$)$_{12}$(OAc)$_{12}$]$^{8+}$	9	n.r.	n.r.	[71]
1	${}^7/_2$	−1.4, −0.6	−9.2	t.w.
2	${}^7/_2$	−1.7, −0.4	−8.6	t.w.

[a] In cm^{-1}, using the $\hat{H} = -2J\hat{S}_i \cdot \hat{S}_j$ convention.

[b] *Abbreviations:* pko = di(2-pyridyl)ketonoxime; heedH$_2$ = N,N-bis(2-hydroxyethyl)-ethylenediamine; 3,4-dpa = 3,4-dichlorophenoxy acetate; edteH$_4$ = N,N,N′,N′-tetrakis (2-hydroxyethyl)ethylenediamine; thmeH$_3$ = 1,1,1-tris(hydroxymethyl)ethane; teaH$_3$ = triethanolamine; (peolH$_4$ = pentaerythritol (C(CH$_2$OH)$_4$); bpy = 2,2′-bipyridine; n.r. = not reported; t.w. = this work.

entries in Table 5. Taking this interaction as J_d, we repeated the simulations and found that an equally good fit of all data could be obtained with a **F** J_d interaction. The simulation parameters were $J_a = -9.7\ cm^{-1}$, $J_b = -0.6\ cm^{-1}$, $J_c = -1.3\ cm^{-1}$ and $J_d = +0.9\ cm^{-1}$ for **1**·2H_2O, and $J_a = -7.3\ cm^{-1}$, $J_b = -0.9\ cm^{-1}$, $J_c = -0.7\ cm^{-1}$ and $J_d = +0.3\ cm^{-1}$ for **2**·2H_2O, with a fixed $g = 2.0$. We thus cannot rule out that the oximate-bridged $Mn^{II}Mn^{II}$ pair is very weakly **F**, but we can conclude that the coupling between Mn5A and the other Mn^{II} ions is dominantly **AF**.

4. Conclusions

Two new Mn_5 clusters have been obtained from aerial oxidation of a Mn^{II} reaction system in MeOH with two types of chelates. **1** and **2** join only a small family of complexes containing only Mn^{II} and Mn^{IV}. This work emphasizes the often complicated *in situ* ligand transformations that can occur, in this case leading to products containing two unusual hemiacetal chelates. The complexes both have an $S = {}^7/_2$ ground state resulting from **AF** $Mn^{II}Mn^{IV}$ interactions frustrating weaker **AF** $Mn^{II}Mn^{II}$ interactions.

Acknowledgment

This work was supported by the US National Science Foundation (Grant CHE-1565664).

Appendix A. Supplementary data

CCDC 1498988 contains the supplementary crystallographic data for **1** *x*MeOH·*y*H_2O. These data can be obtained free of charge via http://www.ccdc.cam.ac.uk/conts/retrieving.html, or from the Cambridge Crystallographic Data Centre, 12 Union Road, Cambridge CB2 1EZ, UK; fax: (+44) 1223-336-033; or e-mail: deposit@ccdc.cam.ac.uk. Supplementary data associated with this article can be found, in the online version, at http://dx.doi.org/10.1016/j.poly.2016.10.018.

References

[1] R.M. Cinco, A. Rompel, H. Visser, G. Aromi, G. Christou, K. Sauer, M.P. Klein, V.K. Yachandra, Inorg. Chem. 38 (1999) 5988.
[2] V.K. Yachandra, K. Sauer, M.P. Klein, Chem. Rev. 96 (1996) 2927.
[3] K.N. Ferreira, T.M. Iverson, K. Maghlaoui, J. Barber, S. Iwata, Science 303 (2004) 1831.
[4] K.D. Karlin, Science 262 (1993) 1499.
[5] B.L. Vallee, R.J.P. Williams, Proc. Nat. Acad. Sci. U.S.A. 59 (1968) 498.
[6] D. Gatteschi, L. Bogani, A. Cornia, M. Mannini, L. Sorace, R. Sessoli, Solid State Sci. 10 (2008) 1701.
[7] H.A. Jahn, E. Teller, Proc. R. Soc. Lond., Ser. A 161 (1937) 220.
[8] M.A. Halcrow, Chem. Soc. Rev. 42 (2013) 1784.
[9] G. Christou, D. Gatteschi, D. Hendrickson, R. Sessoli, MRS Bull. 25 (2000) 66.
[10] J. Friedman, M. Sarachik, J. Tejada, R. Ziolo, Phys. Rev. Lett. 76 (1996) 3830.
[11] D. Gatteschi, R. Sessoli, Angew. Chem., Int. Ed. 42 (2003) 268.
[12] W. Wernsdorfer, R. Sessoli, A. Caneschi, D. Gatteschi, A. Cornia, J. Phys. Soc. Jpn. 69 (2000) 375.
[13] W. Wernsdorfer, R. Sessoli, Science 284 (1999) 133.
[14] W. Wernsdorfer, M. Soler, G. Christou, D.N. Hendrickson, J. Appl. Phys. 91 (2002) 7164.
[15] M. Urdampilleta, S. Klyatskaya, J.P. Cleuziou, M. Ruben, W. Wernsdorfer, Nat. Mater. 10 (2011) 502.
[16] L. Bogani, W. Wernsdorfer, Nat. Mater. 7 (2008) 179.
[17] W. Wernsdorfer, Int. J. Nanotechnol. 7 (2010) 497.
[18] N.C. Harden, M.A. Bolcar, W. Wernsdorfer, K.A. Abboud, W.E. Streib, G. Christou, Inorg. Chem. 42 (2003) 7067.
[19] T.C. Stamatatos, K.A. Abboud, W. Wernsdorfer, G. Christou, Angew. Chem., Int. Ed. 45 (2006) 4134.
[20] T.C. Stamatatos, D. Foguet-Albiol, S.C. Lee, C.C. Stoumpos, C.P. Raptopoulou, A. Terzis, W. Wernsdorfer, S.O. Hill, S.P. Perlepes, G. Christou, J. Am. Chem. Soc. 129 (2007) 9484.
[21] T.C. Stamatatos, K.A. Abboud, W. Wernsdorfer, G. Christou, Angew. Chem., Int. Ed. 46 (2007) 884.
[22] H.S. Wang, Z.C. Zhang, X.J. Song, J.W. Zhang, H.B. Zhou, J. Wang, Y. Song, X.Z. You, Dalton Trans. 40 (2011) 2703.
[23] T. Taguchi, W. Wernsdorfer, K.A. Abboud, G. Christou, Inorg. Chem. 49 (2010) 10579.
[24] T. Taguchi, M.R. Daniels, K.A. Abboud, G. Christou, Inorg. Chem. 48 (2009) 9325.
[25] D.I. Alexandropoulos, M.J. Manos, C. Papatriantafyllopoulou, S. Mukherjee, A.J. Tasiopoulos, S.P. Perlepes, G. Christou, T.C. Stamatatos, Dalton Trans. 41 (2012) 4744.
[26] C.J. Milios, E. Kefalloniti, C.P. Raptopoulou, A. Terzis, R. Vicente, N. Lalioti, A. Escuer, S.P. Perlepes, Chem. Commun. (2003) 819.
[27] M. Holynska, S. Dehnen, Inorg. Chem. Commun. 14 (2011) 1290.
[28] T.C. Stamatatos, B.S. Luisi, B. Moulton, G. Christou, Inorg. Chem. 47 (2008) 1134.
[29] A. Escuer, B. Cordero, M. Font-Bardia, T. Calvet, O. Roubeau, S.J. Teat, S. Fedi, F.F. de Bianie, Dalton Trans. 39 (2010) 4817.
[30] S. Khanra, T. Weyhermuller, P. Chaudhuri, Dalton Trans. (2008) 4885.
[31] H. Hiraga, H. Miyasaka, K. Nakata, T. Kajiwara, S. Takaishi, Y. Oshima, H. Nojiri, M. Yamashita, Inorg. Chem. 46 (2007) 9661.
[32] L. Lecren, W. Wernsdorfer, Y.G. Li, O. Roubeau, H. Miyasaka, R. Clerac, J. Am. Chem. Soc. 127 (2005) 11311.
[33] T.C. Stamatatos, K.M. Poole, K.A. Abboud, W. Wernsdorfer, T.A. O'Brien, G. Christou, Inorg. Chem. 47 (2008) 5006.
[34] D.C. Li, H.S. Wang, S.N. Wang, Y.P. Pan, C.J. Li, J.M. Dou, Y. Song, Inorg. Chem. 49 (2010) 3688.
[35] J. Cano, T. Cauchy, E. Ruiz, C.J. Milios, C.C. Stoumpos, T.C. Stamatatos, S.P. Perlepes, G. Christou, E.K. Brechin, Dalton Trans. (2008) 234.
[36] T.C. Starnatatos, D. Foguet-Albiol, C.C. Stoumpos, C.P. Raptopoulou, A. Terzis, W. Wernsdorfer, S.P. Perlepes, G. Christou, J. Am. Chem. Soc. 127 (2005) 15380.
[37] A.M. Mowson, T.N. Nguyen, K.A. Abboud, G. Christou, Inorg. Chem. 52 (2013) 12320.
[38] T.N. Nguyen, W. Wernsdorfer, M. Shiddiq, K.A. Abboud, S. Hill, G. Christou, Chem. Sci. 7 (2016) 1156.
[39] T.N. Nguyen, W. Wernsdorfer, K.A. Abboud, G. Christou, J. Am. Chem. Soc. 133 (2011) 20688.
[40] T.N. Nguyen, M. Shiddiq, T. Ghosh, K.A. Abboud, S. Hill, G. Christou, J. Am. Chem. Soc. 137 (2015) 7160.
[41] C.J. Milios, T.C. Stamatatos, S.P. Perlepes, Polyhedron 25 (2006) 134.
[42] D. Olbert, H. Goerls, D. Conrad, M. Westerhausen, Eur. J. Inorg. Chem. (2010) 1791.
[43] R.C. Weast, CRC Handbook of Chemistry and Physics, CRC Press Inc., Boca Raton, FL, 1984.
[44] Bruker, SAINT, 6.36a; Bruker AXS Inc., Madison, WI, 1998.
[45] E.C. Yang, N. Harden, W. Wernsdorfer, L. Zakharov, E.K. Brechin, A.L. Rheingold, G. Christou, D.N. Hendrickson, Polyhedron 22 (2003) 1857.
[46] (a) C.D. Hurd, J. Chem. Educ. 43 (1966) 527;
(b) L.M. Azofra, I. Alkorta, J. Elguero, A. Toro-Labbe, J. Phys. Chem. A 116 (2012) 8250;
(c) Jonathan Clayden, Nicken Greeves, S. Warren, 2nd ed., Oxford University Press, 2012.
[47] E.C. Sanudo, E.K. Brechin, C. Boskovic, W. Wernsdorfer, J. Yoo, A. Yamaguchi, T. R. Concolino, K.A. Abboud, A.L. Rheingold, H. Ishimoto, D.N. Hendrickson, G. Christou, Polyhedron 22 (2003) 2267.
[48] (a) A.N. Georgopoulou, C.G. Efthymiou, C. Papatriantafyllopoulou, V. Psycharis, C.P. Raptopoulou, M. Manos, A.J. Tasiopoulos, A. Escuer, S.P. Perlepes, Polyhedron 30 (2011) 2978;
(b) A.A. Kitos, C.G. Efthymiou, M.J. Manos, A.J. Tasiopoulos, V. Nastopoulos, A. Escuer, S.P. Perlepes, Dalton Trans. 45 (2016) 1063;
(c) H. Sartzi, C.C. Stoumpos, M. Giouli, I.I. Verginadis, S.C. Karkabounas, L. Cunha-Silva, A. Escuer, S.P. Perlepes, Dalton Trans. 41 (2012) (1988) 11984;
(d) T.C. Stamatatos, C.G. Efthymiou, C.C. Stoumpos, S.P. Perlepes, Eur. J. Inorg. Chem. (2009) 3361;
(e) T.C. Stamatatos, V. Tangoulis, C.P. Raptopoulou, A. Terzis, G.S. Papaefstathiou, S.P. Perlepes, Inorg. Chem. 47 (2008) 7969;
(f) C.C. Stoumpos, O. Roubeau, G. Aromi, A.J. Tasiopoulos, V. Nastopoulos, A. Escuer, S.P. Perlepes, Inorg. Chem. 49 (2010) 359.
[49] C. Boskovic, W. Wernsdorfer, K. Folting, J.C. Huffman, D.N. Hendrickson, G. Christou, Inorg. Chem. 41 (2002) 5107.
[50] W. Ouellette, B.S. Hudson, J. Zubieta, Inorg. Chem. 46 (2007) 4887.
[51] C.J. Matthews, L.K. Thompson, S.R. Parsons, Z.Q. Xu, D.O. Miller, S.L. Heath, Inorg. Chem. 40 (2001) 4448.
[52] S. Brooker, V. McKee, T. Metcalfe, Inorg. Chim. Acta 246 (1996) 171.
[53] C.J. Matthews, Z.Q. Xu, S.K. Mandal, L.K. Thompson, K. Biradha, K. Poirier, M.J. Zaworotko, Chem. Commun. (1999) 347.
[54] M. Wang, C.-B. Ma, D.-Q. Yuan, H.-S. Wang, C.-N. Chen, Q.-T. Liu, Inorg. Chem. 47 (2008) 5580.
[55] P.-P. Yang, X.-Y. Song, R.-N. Liu, L.-C. Li, D.-Z. Liao, Dalton Trans. 39 (2010) 6285.
[56] M.S. Lah, V.L. Pecoraro, J. Am. Chem. Soc. 111 (1989) 7258.
[57] C. Dendrinou-Samara, A.N. Papadopoulos, D.A. Malamatari, A. Tarushi, C.P. Raptopoulou, A. Terzis, E. Samaras, D.P. Kessissoglou, J. Inorg. Biochem. 99 (2005) 864.
[58] C.-I. Yang, W. Wernsdorfer, G.-H. Lee, H.-L. Tsai, J. Am. Chem. Soc. 129 (2007) 456.
[59] T.C. Stamatatos, K.A. Abboud, G. Christou, Dalton Trans. (2009) 41.
[60] T. Shiga, H. Oshio, Polyhedron 26 (2007) 1881.
[61] C.P. Berlinguette, D. Vaughn, C. Canada-Vilalta, J.R. Galan-Mascaros, K.R. Dunbar, Angew. Chem., Int. Ed. 42 (2003) 1523.

[62] R.A. Reynolds, D. Coucouvanis, Inorg. Chem. 37 (1998) 170.
[63] K. Kambe, J. Phys. Soc. Jpn. 5 (1950) 48.
[64] J.J. Borras-Almenar, J.M. Clemente-Juan, E. Coronado, B.S. Tsukerblat, J. Comput. Chem. 22 (2001) 985.
[65] C.C. Stoumpos, T.C. Stamatatos, H. Sartzi, O. Roubeau, A.J. Tasiopoulos, V. Nastopoulos, S.J. Teat, G. Christou, S.P. Perlepes, Dalton Trans. (2009) 1004.
[66] G. Karotsis, L.F. Jones, G.S. Papaefstathiou, A. Collins, S. Parsons, T.D. Nguyen, M. Evangelisti, E.K. Brechin, Dalton Trans. (2008) 4917.
[67] A.J. Zhou, J.L. Liu, R. Herchel, J.D. Leng, M.L. Tong, Dalton Trans. (2009) 3182.
[68] T. Afrati, C. Dendrinou-Samara, C.R. Raptopoulou, A. Terzis, V. Tangoulis, D.P. Kessissoglou, Angew. Chem., Int. Ed. 41 (2002) 2148.
[69] C.J. Millos, S. Piligkos, A.R. Bell, R.H. Laye, S.J. Teat, R. Vicente, E. McInnes, A. Escuer, S.P. Perlepes, R.E.P. Winpenny, Inorg. Chem. Commun. 9 (2006) 638.
[70] S.K. Langley, N.F. Chilton, B. Moubaraki, K.S. Murray, Dalton Trans. 41 (2012) 9789.
[71] R.T.W. Scott, S. Parsons, M. Murugesu, W. Wernsdorfer, G. Christou, E.K. Brechin, Angew. Chem., Int. Ed. 44 (2005) 6540.